



Surgical management of Osteochondral Lesions of the Talus

Thesis

*Submitted for partial fulfillment of M.D degree in
Orthopedic Surgery*

By

Mohammed Elsayed Kamel

M.B.B.Ch., M. Sc. Of Orthopaedic Surgery

Supervised by

Professor Dr. Hesham Ahmed Fahmy

Professor of Orthopaedic Surgery

Ain Shams University

Dr. Waleed Elsayed Elshabrawy

Lecturer of Orthopaedic Surgery

Ain Shams University

Dr. Mohammed Mokhtar Abdella

Lecturer of Orthopaedic Surgery

Ain Shams University

Faculty of Medicine

Ain-Shams University

2015

Acknowledgements

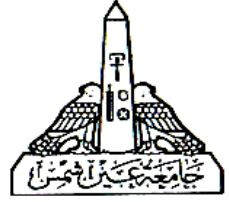
My gratitude and appreciation to **Prof. Dr. Hesham Fahmy**, Professor of Orthopaedics, Ain Shams University for his valuable supervision and generous support. I can't thank him enough for his advice and suggestions on all aspects of this thesis and my career.

Many thanks for **Prof. Dr. Ezzat Mohammed Kamel**, Professor of orthopaedic surgery, Ain Shams University, for his most valuable guidance, unlimited patience and efforts to teach me arthroscopic assisted surgery.

I would like to express my deepest thanks to **Dr. Waleed Elshabrawy**, Lecturer of Orthopedics, Ain Shams University for his assistance, effort and advice during this study.

Special thanks must go to **Dr. Mohammed Mokhtar**, Lecturer of Orthopaedics, Ain Shams University. Without his expert help and assistance I would have been unable to undertake such a project. I am deeply grateful to him for all what he had done for me.

As I would like to thank **Prof. Dr. Xavier Oliva** from Spain, from whom I saw the technique of bone graft sealed with periosteal patch using *GLUBRAN for the first time*



المعالجة الجراحية لمرض الاصابة العظمية الغضروفية لعظمة القنزعه

بحث مقدم توطئة للحصول على درجة الدكتوراة فى جراحة العظام

مقدمة من

طبيب/ محمد السيد كامل
ماجستير جراحة العظام
جامعة عين شمس - كلية الطب

تحت إشراف

الأستاذ الدكتور/ هشام احمد فهمي
أستاذ جراحة العظام
كلية الطب - جامعة عين شمس

الدكتور/ وليد السيد الشبراوي
مدرس جراحة العظام
كلية الطب - جامعة عين شمس

الدكتور/ محمد مختار عبد اللا
مدرس جراحة العظام
كلية الطب - جامعة عين شمس

كلية الطب
جامعة عين شمس

2015

CONTENTS

	Page
LIST OF FIGURES	i
LIST OF TABLES	ix
LIST OF ABBREVIATIONS.....	x
APPENDIX	xi
INTRODUCTION.....	1
AIM OF THE WORK.....	4
REVIEW OF LITERATURE	
BASIC SCIENCE.....	5
PATHOLOGY	20
DIAGNOSIS	60
CLASSIFICATIONS	86
TREATMENT	90
PATIENTS AND METHODS.....	140
RESULTS.....	161
DISCUSSION.....	171
CONCLUSION.....	201
SUMMARY	202
REFERENCES.....	204
ARABIC SUMMARY	-

LIST OF FIGURES

Fig. No.	Title	Page
(1-1)	Microscopic picture of articular cartilage	5
(1-2)	Arthroscopic picture of normal articular cartilage	6
(1-3)	Microscopic picture for zones of articular cartilage	7
(1-4)	Schematic drawing for the different collagen orientation in different zones of articular cartilage	7
(1-5)	Microscopic picture of tidemark	8
(1-6)	EM pictures of the osteochondral junction	10
(1-7)	Schematic diagrams showing normal anatomy of ankle cartilage, subchondral plate and subchondral bone area	14
(1-8)	Schematic diagram for an aggrecan and proteoglycan aggregate	15
(1-9)	Schematic diagram comparing the deformation of the cartilage in a congruent (ankle) and incongruent (knee) joint	18
(2-1)	MRI and SPECT of symptomatic and asymptomatic OLTs in same ankle	25
(2-2)	Nine-zone anatomic grid of talar dome surface	26
(2-3)	Coronal ankle MRI images and corresponding arthroscopic picture of uncontained medial OLT	27
(2-4)	Coronal Ankle MRI images and corresponding arthroscopic picture of Contained medial OLT	27
(2-5)	Schematic diagram of bone bruises	31
(2-6)	Schematic drawing of Subchondral microfracture	32
(2-7)	MRI images showing Posteromedial talar bruise	32
(2-8)	schematic drawing of Subchondral impaction (geographic, crescentic, linear type)	33
(2-9)	Sagittal ankle MRI images showing geographic talar bone bruise: A Sagittal T1-weighted SE image B sagittal STIR image (B) (69)	33

Fig. No.	Title	Page
(2-10)	Schematic drawing of Acute injury of the articular surface with disrupted cartilage (chondral, osteochondral lesions)	34
(2-11)	MRI image of an osteochondral fragmen	34
(2-12)	Osteochondral plug harvested from the center of the lesion	37
(2-13)	Histological sections of normal knee and OCD I	39
(2-14)	Histological section of ICRS grade III lesion	39
(2-15)	Schematic diagrams showing a loose osteochondralfragment	46
(2-16)	Coronal ankle MRI showing subchondral cyst	49
(2-17)	A case of cystic lesion with corresponding arthroscopic picture	50
(2-18)	CT reveals cystic lesion . Operative procedure of the same medial osteochondral lesion of the talus	50
(2-19)	Sagittal T2-weighted MRI study of an ankle with an OLT	52
(2-20)	Roughened cartilage surface	56
(2-21)	Superficial flap and fissures present at the base	56
(2-22)	Coronal MRI ankle (high resolution) showing osteochondral junction separation	57
(2-23)	Chondral Flap characterized by the detachment of a portion of the articular cartilage without subchondral bone	58
(2-24)	Full thickness anterior cartilage defect extending from the medial to lateral aspect of the talar dome	58
(3-1)	Lateral and anteroposterior radiographs of a medial talar dome lesion	66
(3-2)	Antero-posterior radiographs showing bilateral OLT affecting the medial dome of the talus	66
(3-3)	radiographic Saltzman view for hindfoot malalignment	67
(3-4)	AP and lateral ankle PXR's showing stress views for ankle instability	67

Fig. No.	Title	Page
(3-5)	an arthro CT image showing a cartilage fissure	68
(3-6)	schematic drawing of Ferkel CT classification	70
(3-7)	CT image of osteochondral fragment with its corresponding arthroscopic picture	70
(3-8)	Chondral separated lesion : CT subchondral findings in: sclerosis, microcyst, honeycomb and large cyst with corresponding arthroscopic cartilage lesions	71
(3-9)	Classification of CT findings based on subchondral bone findings in OLTs	72
(3-10)	A CT of cystic lesion with corresponding arthroscopic view	72
(3-11)	CT coronal image of osteochondral fragment that is not modified	73
(3-12)	coronal CT image showing fragmentation and increased density of fragment	73
(3-13)	CT images of osteochondral fragment in which fragment is resorbed	74
(3-14)	CT images of subchondral cyst and their relation to joint cavity	74
(3-15)	CT image of an OLT(arrow) located medial in the talar dome	75
(3-16)	Comparison of image quality using 1.5 and 3 T MRI	77
(3-17)	Sagittal MRI shows thin fibrillated cartilage	78
(3-18)	coronal MRI ankle (high resolution) showing osteochondral junction separation	79
(3-19)	MRI images Minimally displaced chondral flap midlateral talar dome	80
(3-20)	coronal ankle MRI showing displaced chondral fracture with resultant full thickness chondral defect	80
(3-21)	MRI image showing in situ unstable osteochondral lesion with underlying cystic change	82

Fig. No.	Title	Page
(3-22)	MRI image of insitu fragment	83
(3-23)	In situ osteochondral lesion with confluent fluid signal intensity at the interface between the osteochondral fragment and the base of the potential osteochondral crater	83
(3-24)	medial osteochondral fragment	84
(3-25)	Displaced medial osteochondral fragment	84
(3-26)	sagittal MRI showing large cystic, subchondral changes	85
(3-27)	Chronic medial talar dome osteochondral lesion, with 1.3 cm subchondral cyst containing fibrotic debris	85
(3-28)	showing A Sagittal T2-weighted MRI study of an ankle with a reticular bone bruise	86
(3-29)	showing Osteochondral lesion associated with collapse of the subchondral bone and overlying cartilage hypertrophy	87
(4-1)	Schematic drawing for Berndt and Harty classification	92
(5-1)	schematic drawings of an ankle, showing the different medial malleolar osteotomy techniques	94
(5-2)	Arthroscopic view of a lateral talar cartilage lesion as seen from anteromedial portal before and after debridement	97
(5-3)	arthroscopic view of the same defect as fig 5-1 after microfracture	97
(5-4)	arthroscopic view of a chondral defect treated with a microfracture awl	98
(5-5)	arthroscopic image demonstrating transmalleolar drilling of medial OLT with Microvector drill guide through the anteromedial portal	98
(5-6)	fluoroscopic image showing retrograde drilling of medial OLT using K-wire	99
(5-7)	coronal cartilage-sensitive fast-spin ankle MRI of OLT : (A) before and (B) after treatment with OATS	103

Fig. No.	Title	Page
(5-8)	Osteochondral autograft reconstruction from the knee technique	104
(5-9)	Autologous chondrocyte implantation	112
(5-10)	Schematic drawing of the sandwich procedure	114
(5-11)	Allograft Plug Technique	118
(5-12)	Bulk allograft technique	119
(5-13)	Modified mosaicplasty procedure	123
(5-14)	Harvest of osteoperiosteal graft from distal tibia	123
(5-15)	Pre and postoperative MRI for OLT treated with osteoperiosteal graft	125
(5-16)	Comparison of chondrocyte density and GAG production between adult and juvenile chondrocyte	126
(5-17)	DeNovo NT (Zimmer, Inc, Warsaw,IN)	127
(5-18)	Pre and postoperative MRI of OLT treated with PJCAT	128
(5-19)	Open PJCAT procedure	128
(5-20)	Arthroscopic PJCAT procedure	129
(5-21)	Open AMIC procedure	133
(5-22)	Hemicap	134
(5-23)	Biopoly	135
(5-24)	TRUFIT CB	135
(5-25)	Bone marrow concentrate	136
(5-26)	PRP	138
(6-1)	How lesion dimensions are calculated on MRI	146
(6-2)	How lesion area calculated	146
(6-3)	Localisation of anterolateral portal	150
(6-4)	Differentiation between healthy and diseased cartilage	151
(6-5)	Arthroscopic measurment of cartilage defect using graduated	151

Fig. No.	Title	Page
	probe	
(6-6)	Arthroscopic view of Cartilage defect after debridment	152
(6-7)	Arthroscopic view of K-wire drilling	153
(6-8)	Arthroscopic view of 2 drill holes	153
(6-9)	Arthroscopic view showing fat globules escaping from drilling holes	154
(6-10)	Fluoroscopic view of retrograde drilling	154
(6-11)	Medial Ankle approach	155
(6-12)	Medial Malleolar Osteotomy	156
(6-13)	Curretage and drilling of subchondral cyst	156
(6-14)	Periosteal patch harvest	157
(6-15)	Autologus cancellous Bone graft haevest	157
(6-16)	Application of bone graft	158
(6-17)	Application of glue	158
(6-18)	Sealing the defect with periosteal patch	159
(6-19)	Periosteal patch is stable	159
(6-20)	Closure of malleolar osteotomy with 2 screws	160
(6-21)	Fluoroscopic image for closure of ostetomy with screws	160
(7-1)	Pie chart diagram showing the percentage of traumatic OLT	165
(7-2)	Sagittal MRI ankle showing examples of small and large cystic lesions	165
(7-3)	Examples of medial and lateral lesions	166
(7-4)	Example of uncontained lesion	166
(7-5)	Pie chart showing the distribution of subchondral features	167
(7-6)	Different examples of subchondral features	167
(7-7)	an error bar chart showing the significant improvement in the mean postoperative AOFAS score	168

Fig. No.	Title	Page
(7-8)	A bar chart comparing the improvement between both techniques	169
(7-9)	A pie chart showing the grading of results among the study population	169
(7-10)	Pie chart showing the distribution of good, fair and poor results	170
(7-11)	A bar chart comparing the improvement in AOFAS scores between traumatic and non-traumatic lesions	172
(7-12)	A bar chart comparing the improvement in postoperative AOFAS score between contained and uncontained lesions	173
(7-13)	A bar chart comparing the improvement in postoperative AOFAS score in different types of subchondral lesions	174
(7-14)	AP and oblique view PXR showing medial cystic lesion	175
(7-15)	coronal and sagittal MRI showing centromedial cystic lesion with high signal intensity	176
(7-16)	8 month Postoperative AP and Lat PXR note the resolution of medial cyst on AP view in comparison to preoperative AP	176
(7-17)	12 month postoperative coronal and sagittal ankle MRI: showing the cyst is filled with low intensity on coronal MRI denoting fibrosis and on sagittal STIR view the cyst decreased in size, yet still there is increased intensity	177
(7-18)	bilateral standing Ankle AP PXR showing cystic medial lesion on the left talus	178
(7-19)	preoperative coronal and sagittal ankle MRI showing medial cystic lesion with increased signal intensity	179
(7-20)	14 month Postoperative ankle AP PXR showing healing of osteotomy site and complete resolution of cyst	180
(7-21)	Preoperative coronal and axial CT of subchondral cyst	181
(7-22)	Preoperative coronal and axial CT for the same lesion showing resolution of cyst	182

Fig. No.	Title	Page
(7-23)	Preoperative ankle PXR showing no obvious abnormality	184
(7-24)	Preoperative ankle MRI showing medial bone marrow edema	184
(7-25)	Postoperative ankle MRI showing resolution of the edema	185
(8-1)	Correlation between defect size and clinical outcome	190
(8-2)	Histological appearance of a core biopsy taken from the centre of the talar defect	193
(8-3)	Bar chart showing the mean postoperative AOFAS score of studies treating OLT with bone marrow stimulation compared to the current study	196
(8-4)	Bar chart comparing results of bone graft with periosteum with results of other studies reporting treatment of OLT with OATS	197
(8-5)	Bar chart showing the results of current study in comparison with other studies reporting result of treating OLT using ACI	199

LIST OF TABLES

Table. No.	Title	Page
1-1	comparison between different zones of articular cartilage	7
4-1	Radiographic (PXR and CT) classification systems reported in literature	89
4-2	MRI classification systems reported in literature	90
4-3	Specific and non specific arthroscopic classification systems reported in literature	91
5-1	Approaches for Medial and Lateral lesions	94
5-2	List of published studies reporting results of marrow stimulation in management of OLT	100
5-3	List of studies reporting results of OATS in management of OLT	107
5-4	List of studies reporting results of ACI in management of OLT	115
7-1	correlation between gender and AOFAS scores	171
7-2	correlation between lesion containment and AOFAS scores	173
7-3	correlation between lesion type and AOFAS scores	173
7-4	correlation between site of lesion and AOFAS scores	171
8-1	showing comparison of patient characteristics between the current study and previous studies in 2 systematic reviews	187

LIST OF ABBREVIATIONS

ACI	Autologus Chondrocyte Implantation
AMIC	Autologus Membrane Induced Chondrogenesis
AOFAS	American Orthopaedic Foot and Ankle Society
AOFAS score	American Orthopaedic Foot and Ankle Society (AOFAS) Ankle-Hindfoot Score
AVN	Avascular necrosis
BME	Bone Marrow Edema
BMDCT	Bone Marrow Derived Cells Transplantation
CT	Computed Tomography
dGEMRIC	delayed Gadolinium-enhanced MRI of Cartilage
EMA	European Medicines Agency
EM	Electron Microscope
FDA	US Food and Drug Administration
HA	Hyaluronic acid
GAGs	Glycosaminoglycans
HLA	Human Leucocytic Antigen
MACI	Matrix-induced Autologous Chondrocyte Implantation
MSAC	Medical services advisory committee
MRI	Magnetic Resonance Imaging
OATS	Osteochondral Autograft Transfer System or Osteoarticular Transfer System
OCD	Osteochondritis dissecans or Osteochondral Defect
OLT	Oseochondral Lesion of Talar dome
PJCAT	Particulated juvenile cartilage allograft transplantation
PXR	Plain X-ray
RF	Radio Frequency
ROM	Range Of Motion
SPECT	Single-photon emission computed tomography
STIR	short tau inversion recovery

APPENDIX

AOFAS Hindfoot score

Ankle-Hindfoot Scale (100points Total)

I Pain (40 points)

None	40
Mild, occasional	30
Moderate, daily	20
Severe, almost always present	0

II Function (50 points)

Activity limitations, support requirement	
No limitations, no support	10
No limitation of daily activities, limitation of recreational activities, no support	7
Limited daily and recreational activities, cane	4
Severe limitation of daily and recreational activities, walker, crutches, wheelchair, brace	0

Maximum walking distance, blocks	
Greater than 6	5
4-6	4
1-3	2
Less than 1	0

Walking surfaces	
No difficulty on any surface	5
Some difficulty on uneven terrain, stairs, inclines, ladders	3
Severe difficulty on uneven terrain, stairs, inclines, ladders	0